Northumbria Research Link

Check for updates

Soft diamond-like carbon coatings with superior biocompatibility for medical applications

Abdul Wasy Zia [a,*], Ioannis Anestopoulos [b,c], Mihalis I. Panayiotidis [b,c], Martin Birkett [a]

[a] *Faculty of Engineering and Environment, Northumbria University, United Kingdom*
[b] *Department of Cancer Genetics, Therapeutics & Ultrastructural Pathology, The Cyprus Institute of Neurology & Genetics, Nicosia, Cyprus*
[c] *The Cyprus School of Molecular Medicine, The Cyprus Institute of Neurology and Genetics, Nicosia, Cyprus*

ARTICLE INFO

ABSTRACT

Biomedical applications of diamond-like carbon (DLC) coatings are continuously increasing due to their superior mechanical properties, low friction coefficient, antiwear characteristics, and biocompatibility. The mechanical and tribological characteristics of DLC coatings have been comprehensively investigated on various substrate systems as a function of their deposition parameter dependant features for various biomaterial applications. However, the relationship between biocompatibility and resulting hardness of DLC coatings as a function of their bias voltage driven intrinsic features like sp^2 and sp^3 bonds remains largely unexplored. In this work, a series of DLC coatings are prepared as a function of varying bias voltage from 0 to −120 V, and characterised for their atomic structure, physical, and mechanical properties, and biocompatibility. The contact angle and surface roughness of the DLC coatings reduce while hardness increases from 7.8 to 20.3 GPa with increasing bias voltage from 0 to −120 V. A relatively soft DLC coating is shown to retain excellent biocompatibility which is approximately 38% higher than the harder DLC coatings following exposure of their leached extracts to L929 mouse fibroblast cells. This work demonstrates the complex interdependence of biocompatibility and hardness of DLC coatings and the outcomes will support correct material selection with an appropriate balance of these key properties for specific biomedical applications such as load-carrying and non-load carrying devices.

1. Introduction

Diamond-like carbon (DLC) coatings are recognised for their superior mechanical properties, low friction coefficient, antiwear characteristics, and biocompatibility. Amorphous carbon has shown bio-inertness in simulated body fluid [1], non-toxic response towards osteoblast-like cells [2], *in vitro* growth and biomineralisation of human osteoblast [3]. These coatings have also shown a reduction in skin tear when used for invasive surgery devices and tools [4]. Hence, DLC coatings are widely used for biomedical applications such as surgical tools and medical devices, and their usage has been continuously increasing in recent years, particularly for invasive implants. These coatings are being used for heart valves [5], heart diaphragms [6], stents [7], catheters [8], dental implants [9,10], and intraocular lenses [11], etc. Specifically, DLC coatings are receiving wide attention for load-carrying orthopaedic joints, i.e., knee and hip joints [12,13]. Applying DLC coatings to *in vivo* bearing interfaces of artificial joints increases implant performance and useable life due to minimised friction and wear rates. DLC coated metal pairs have shown a 100% decline in wear rates compared to metal/metal and metal/polyethylene pairs. Particularly for hip joints, applying DLC coatings on the metallic femoral head has been shown to reduce the wear of plastic acetabular cup by 10 times [14]. Currently, DLC coatings are commercially available for numerous orthopaedic components under different tradenames such as Medthin™ by IHI Ionbond AG, BALIMED™ DLC by Oerlikon Blazers, DYNAMANT™ by Mitsubishi and Carbioceram™ by Lavender Medical Ltd. The DLC applications for biomedical implants are continually increasing for new bio-mechanical products. New intellectual property rights during last three years are documented on joint replacement prosthesis (CN215839717U, 2022), elbow joints (RU208797U1, 2021), artificial bones (CN112190756A, 2021), C-shaped stents (CN112190375A, 2021), ventricular assist devices (US20200237982A1 2020), knee endoprosthesis (RU196932U1, 2020), and vertical spines (RU189886U1, 2019). Moreover, the increasing global review of the DLC market and more than 100% increase in scientific outcomes [15] also reflects its popularity for scientific and commercial purposes.

Hard DLC coatings offer higher scratch resistance, low friction coefficients and wear rates; therefore, they have been mainly adopted for mechanical applications. The higher hardness of DLC coatings has remained desirous since its inception in 1953 by Schmellenmeier [16] and was demonstrated adequately by Aisenberg and Chabot's experiments in 1971 [17] by applying substrate bias. Since its inception, DLC coatings have remained in high demand for mechanical components, and with time, DLC has found new markets in automotive [18], cutting tools [19], electronics [20], textiles [21], and renewable energy [22] sectors. The biocompatibility of DLC coatings was also explored in the early 1990s [23] and is well-described in consolidated review articles from Hauert [24], Roy [25], Grill [26], and others. Commercially, DLC utilisation as a wear-resistant coating for implants was patented by IHI Ionbond AG in 2012 (US10105468B2) and for titanium-based surgical implants by DePuy Synthes Products Inc in 2013 (CA2903775C). Since then, the applications of DLC coatings are continuously expanding in the medical sector.

Most biocompatibility studies of DLC coatings are performed to highlight its superior medical performance over other materials such as stainless steel [27], titanium [28], titanium-nitride, titanium-oxide [29], titanium-carbide [30], alumina oxide [31], zirconia [32], silicon elastomers, polymethyl methacrylate [33], polyurethane [34], cobalt-chrome [35] cobalt-chrome-molybdenum [36], and other alloys [37]. Similarly, the biocompatibility of DLC coatings was investigated as a function of substrate systems or modified versions of DLC coatings, i.e., doping with solid [38] and gaseous [39] elements, physical and chemical treatments, and multilayer structures [40,41]. Fedal et al. [42] have investigated the blood biocompatibility of commercially available DLC coatings (Carbofilm™) for different substrates systems, i.e., stellite, silicon, and polyethylene terephthalate (PET). Their findings suggest that the *in vitro* biocompatibility of DLC is comparable to stellite but significantly improved from bare PET. Similarly, DLC has shown higher osteoblasts adhesion than carbon nitride, stainless steel, and titanium [43]. In the same way, application of DLC on Ti alloy (Ti13Nb13Zr) has shown at least a 100% increase of Vero fibroblast cell adhesion after 24 h, when compared to uncoated Ti alloy [44]. Another study presents the superior adhesion of 3T3 fibroblast cells on pristine DLC coatings compared to amine and dextran treated DLC coatings [45].

However, DLC coatings are rarely investigated for biocompatibility as a function of their intrinsic properties, such as sp^2 and sp^3 structures and hardness. Hard DLC coatings generally demonstrate better mechanical and tribological performance, hence, they are preferred for load-carrying biomechanical applications. However, hard DLC coatings possess high residual stress, and poor toughness at the same time and are likely to undergo brittle failure due to ceramic-like behaviours. The higher hardness of DLC may not be required for non-load carrying implants such as catheters, stents, diaphragms etc. Therefore, systematic investigation of a correlation between DLC hardness and biocompatibility is desirous. Chen et al. have deposited hydrogenated DLC coatings with different sp^3 and sp^2 proportions (hydrogenated DLC includes carbon/carbon and carbon/hydrogen sp^3 bonds) by regulating precursor and process gas flow rates. Their study demonstrates a threshold value of sp^3 to sp^2 proportion (based on ID/IG values), promoting blood platelet adhesion to the DLC surface [46]. Most commercially available DLC films are hydrogenated as they offer less brittleness and relatively lower friction coefficients, potentially increasing coating life. The hydrogen-free DLC coatings offer higher hardness [47], better cell viability [47], and antimicrobial [48] performance than hydrogenated DLC coatings. However, hydrogen-free DLC coatings somewhat compromise durability due to poor toughness. Within hydrogen-free DLC coatings, even the carbon/carbon sp^2 and sp^3 variations have shown differences in DLC hardness as well as biocompatibility. The DLC hardness could be lower than 1 GPa [49] to as high as 80 GPa [50] and is governed by the composition of carbon sp^2 and sp^3 bonds present in the coatings [51], which equally influences their physio-chemical, friction and wear rates, and biocompatibility. Rare findings have shown that relatively hard DLC coatings have presented comparatively higher thrombus formation when compared to its companions [52]. Therfore, Investigating DLC biocompatibility based on their mechanical hardness is desirous in order to recommend their suitability for invasive or non-invasive, load-carrying and non-load carrying implant devices, as well as other emerging medical applications.

This research presents the first study designed to investigate the correlation between hardness and biocompatibility of hydrogen-free DLC coatings. DLC coatings of varying hardness are deposited as a function of bias voltage. The coatings are characterised by atomic structure, surface roughness, water contact angle, and biocompatibility against L929 mouse fibroblast cells. The outcomes of this work will bring new insights into the appropriate selection of DLC hardness for corresponding biomedical applications, particularly for invasive implants.

2. Materials and methods

The specimen preparation and corresponding characterisation of hydrogen-free DLC coatings as a function of hardness are described below.

2.1. Preparing DLC specimens and biological materials

The DLC coatings were deposited on standard laboratory-grade glass slides using a magnetron sputtering system, UDP 350 Teers Coatings, United Kingdom. The glass slides were ultrasonically cleaned, rinsed with ethanol, and dried with pressurised nitrogen before mounting into the deposition chamber having a base pressure of 0.006 Pa. Plasma substrate cleaning was performed for 5 min at a substrate bias voltage of 400 V and a graphite target current of 0.2 A, to remove surface contamination. The DLC coatings were deposited by sputtering a 99.9% pure graphite target at 2.0 A and 680 V, Ar flow rate of 0.3 L/min, substrate rotation of 2 rpm, and a chamber pressure of 0.7 Pa. The substrate bias voltage is a well-established methodology to regulate the DLC coating hardness [53,54]. In this work, a series of DLC specimens were deposited at -0 V, -40 V, -80 V, and -120 V substrate bias to induce an effect of hardness variation.

L929 mouse fibroblast cells were sourced from German Collection of Microorganisms and Cell Cultures GmbH and grown as a monolayer in Dulbeccos's Modified Eagle Medium (DMEM). The DMEM contained 10% fetal bovine serum, 100 µg/ml streptomycin, 100 U/ml penicillin, 2 mM L-glutamine, and high glucose and were incubated at 100% humidity, 37 ^{o}C, and 5% CO_2. L929 cells were grown into 15–20 passages with maximum confluency of 90%. Further, 72 h and 168 h leached extracts of DLC coatings were prepared to analyse their biocompatibility against L929 cells. Pure DMEM and DMEM containing 10% Dimethyl sulfoxide (DMSO) were used as negative and positive liquid controls. Whereas leached extracts form medical-grade titanium and copper were used as negative and positive solid controls. Compound, regents and plasticware used for the cell culture and extract preparation were purchased from Biosera, USA, Sigma-Aldrich, USA, Fluorochem, UK and Corning, USA. More details on the process and materials sourcing are described in our recent studies [55].

2.2. Characterisation of DLC coatings

The phase composition of carbon in DLC coatings was measured with Raman Spectroscopy, Horiba LabRAM HR microscope, using a HeNe gas laser of 632.8 nm wavelength. The instrument was calibrated with a silicon wafer presenting a sharp peak at 520 cm^{-1}. Five Raman acquisitions were performed for each DLC sample from 1000 to 2000 cm^{-1}. The Raman spectra were processed for deconvolution analysis in OriginLab software. The surface roughness was measured with an Atomic Force Microscope, Dimension™ 3100 by Digital Instruments Veeco Metrology Group. Three measurements of each sample were performed across 25 µm^2 and 100 µm^2 surface areas, scanning 512 lines per sample

at a scanning rate of 0.499 Hz. The contact angle measurement of DLC coatings was performed using 2 μL deionized water drops with a Droplet Shape Analyzer, DSA 30 made by KRÜSS GmbH. The contact angle was measured at six different locations for each sample. The hardness and Young's modulus of DLC coatings were measured with a Nanoindenter, Hysitron Ti900 by Bruker Corporation, USA. Each specimen was indented 27 times in load-control mode at 0.5 mN using a Berkovich tip in compliance with ASTM C1327–15. The data were processed using Microsoft Excel to find averages and standard deviations.

L929 mouse fibroblast cells are well-reported to investigate biological performance of DLC coatings [56,57]. The biocompatibility of DLC coatings was measured against L929 cells using the Alamar Blue assay according to ISO 10993 standard [55]. L929 cells were poured into 96 well plate with a density of 2000 cells/well and incubated overnight. The L929 cells were then exposed to the controls, and 72 h and 168 h leached extracts for 72 h in a humidified incubator at 37 °C with 5% CO_2. Further, 01 mg/mL of Resazurin was added to each well at the end of the 72 h period and allowed to incubate for an additional 4 h.

A plate reader, LT5400 by Labtech, UK was used to measure the absorbance of the cells at 570 nm and 600 nm wavelengths and the difference in absorbance was used to calculate optical density and cell viability. The Alamar Blue assay is a quantitative method that enables the analysis of both cell viability and proliferation. It uses the Resazurin dye, a non-toxic reagent that detects metabolically active and consequently live cells. Specifically, Resazurin is used as an oxidation-reduction indicator and as such exhibits colorimetric changes in the appropriate oxidation-reduction range relating to cellular metabolic reduction. Specifically, the reduced form of resazurin, resorufin, is pink and highly fluorescent, and the intensity of fluorescence produced is proportional to the number of living cells. The above colour change and increased fluorescence can be detected using either fluorescence (using an excitation between 530 and 560 nm and an emission at 590 nm) or absorbance (detected at 570 nm – oxidized form and 600 nm - reduced form).

The cell viability of control materials and DLC coatings was calculated using Eq. (1) [58]:

$$\text{Cell Viability} = \frac{\text{Absorbance of test sample} - \text{Absorbance of positive control}}{\text{Absorbance of negative control} - \text{Absorbance of positive control}} \times 100 \qquad (1)$$

3. Results and discussion

3.1. Structural studies of DLC coatings with Raman Spectroscopy

Fig. 1 presents the phase composition of carbon in bias varied DLC coatings performed with Raman spectroscopy. Fig. 1A presents typical Raman spectra of DLC coatings deposited at 0, -40, −80, and −120 V bias voltage. A broad IG peak and shoulder ID peaks can be observed for all DLC coatings irrespective of their bias voltage. Fig. 1B presents the normalized Raman spectra of bias varied DLC coatings and it also presents the corresponding changes in ID peaks as a function of bias voltage. Fig. 1C presents the Gaussian multipeak deconvolution analysis performed to estimate ID and IG peak positions and the full width half maximum (FWHM) of the G peaks. Correspondingly, Fig. 1D presents the ID and IG peak positions and FWHM (G) for all DLC samples. The peak positions correlate atomic structure, graphitic clustering, and disorder in the structure. The ID peak position reflects carbon sp^2 in breathing modes, while the IG peak position indicates the in-plane vibrations of sp^2 atoms [59,60].

The ID and IG peak positions data present two distinct groups, one for the 0 V DLC coatings and the other for the −40 to −120 V DLC coatings. The DLC coating deposited without bias voltage (0 V) presents the least disorder in carbon atomic structure. The increase in ID peak position for 40 V to −120 V bias deposited DLC coatings suggests an increase in carbon disorder in the films. Referring to Ferrari's three-stage model [61,62], the DLC atomic structure transforms from a-C to ta-C with increasing IG peak positions from 1520 to 1575 cm^{-1}, and carbon sp^3 bonds increase from 20 to 85% correspondingly. Hence, it could be inferred that the 0 V DLC coating has more carbon aromatic rings while carbon chain structure and carbon sp^3 bonds increased for

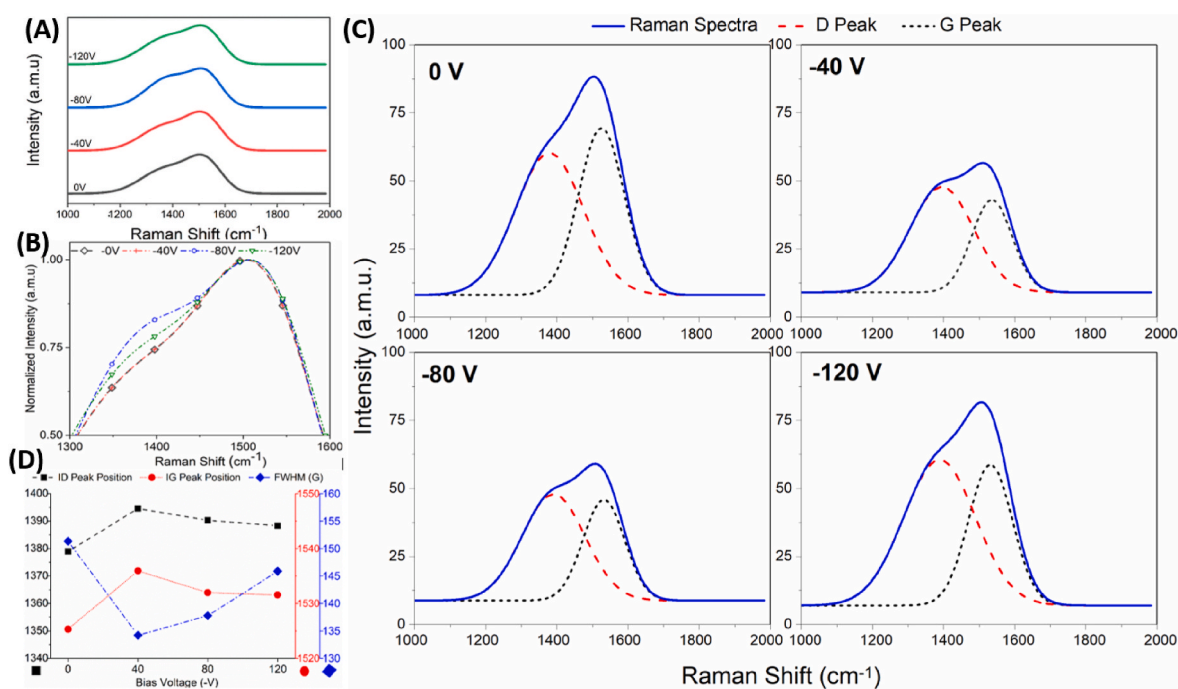**Fig. 1.** Raman Spectroscopy of DLC Coatings deposited as a function of bias voltage. (A) Typical Raman spectra, (B) Normalized Raman spectra presenting variations in ID peak as a function of bias voltage (C) corresponding deconvolution analysis of 0, -40, −80, and −120 V deposited DLC Coatings, and (D) presents ID and IG peak positions and FWHM (G) values obtained from deconvolution analysis.

the −40 to −120 V bias DLC coatings. The relative increase in sp^3 bonds with an application of bias voltage is consistent with previous literature reports [63]. Continuous increase in bias may reverse [61] structural transformation from sp^3 to sp^2 due to relaxing and increased localised thermal kinetics, which is notable for −80 V and −120 V coatings. FWHM (G) correlates with the crystallinity and disorder of carbon atoms. The sharp peaks having lower FWHM are characteristic of crystalline materials, such as a sharp D peak for diamond [64] and a sharp G peak for graphite and graphene [65]. However, the amorphous DLC presents a broad peak [66] with large FWHM values depicting the disordered carbon. The DLC coatings investigated in this study show that the coating made without bias voltage has the highest FHWM (G) values. Whereas, the coating deposited at −40 V has the lowest FWHM (G) value which increases with an increase in bias voltage. This inverse relationship between IG peak position and FWHM (G) is also found in the literature [67,68]. The sp^3 to sp^2 bonds and their transition and disorder in the coating influence the mechanical properties, ion release rates, and biocompatibility of DLC coatings, as discussed in the following sections.

3.2. Contact angle and surface roughness measurement of DLC coatings

Physical properties have a significant impact on the biocompatibility of DLC coatings. Fig. 2 presents the surface roughness of DLC coatings deposited at a bias of 0, -40, −80, and −120 V, scanned for 25 μm^2 surface area. All DLC coatings have a surface roughness of less than 5 nm with a maximum of standard deviation of 5%. Specifically, the arithmetic roughness average of the surface (Ra) was 2.33, 1.75, 1.76, and 1.64 nm and the root mean square of the surface roughness (Rq) was 3.20, 2.25, 2.24, 2.05 nm for coatings deposited at 0, -40, −80, and −120 V bias, when measured across a 25 ± 2 μm^2 surface area. The 100 μm^2 area scanning has also shown consistent trends with Ra values of 2.62, 1.64, 2.88, 1.71 nm and Rq values of 3.61, 2.14, 7.06, and 2.20 nm, respectively. The surface area differences (Rsa) were 0.237%, 0.210%, 0.185%, and 0.173% for the coatings deposited with increasing bias voltage from 0 to −120 V. The continuous reduction of Rsa is potentially due to the thermal migration of carbon atoms whose overall kinetic and thermal energies increase with increasing bias voltage [69] and contribute to smoothening the surface finish.

The micrographs presented in Fig. 2, suggest that the coatings deposited without bias voltage were rougher than the coatings deposited at −40 to −120 V. Considering coating growth behaviours, the absence of bias voltage has a higher probability to transport sp^2 clusters from the sputtering target to the substrate [70]. Whereas, the application of bias

voltage increases the atomic collision and grows fine coating structures on the substrate surface [71]. The surface roughness is reported to control platelet adhesion and their activation on the DLC surface. The rough version of carbon coatings has shown less adherence of platelets and lower activation when compared to smoother DLC coatings [72].

Fig. 3 presents the contact angle measurement of bias varied DLC coatings. In general, all coatings were hydrophilic in nature. Referring to the water contact angle among the DLC coatings, the 0 V specimen has the highest contact angle of 76° which is generally reduced with increasing bias voltage up to −120 V. The −40 V, −80 V, and −120 V specimens have shown a contact angle of 37°, 64°, and 53°, respectively. The contact angle is governed by physio-chemical properties such as surface roughness, surface tension and surface energy, and phase composition of carbon in DLC coatings. It is observed that the DLC coating deposited without bias voltage in the confined experimental design of this study has a higher surface roughness (Ra, Rq, Rsa) when scanned for 25 μm^2 and 100 μm^2 surface areas, and has shown higher
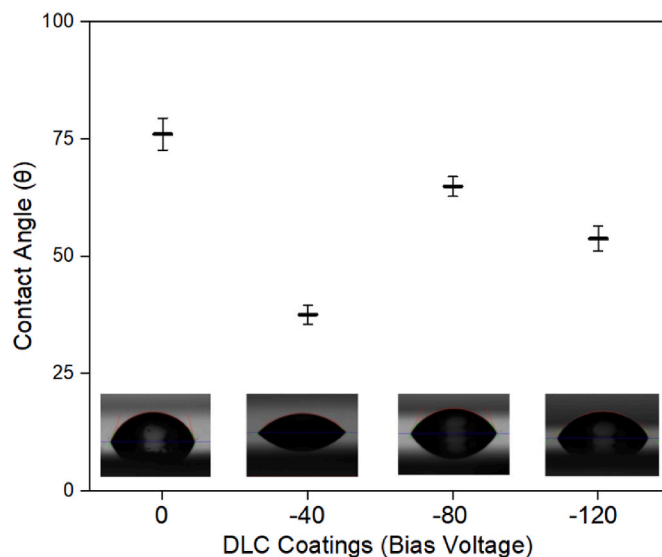
Fig. 3. Water contact angle measurement of DLC coatings deposited on glass substrates as a function of substrate bias voltage. Overall, all the DLC coatings are hydrophobic, while the DLC coating deposited without bias voltage has a higher water contact angle than the biased ones.

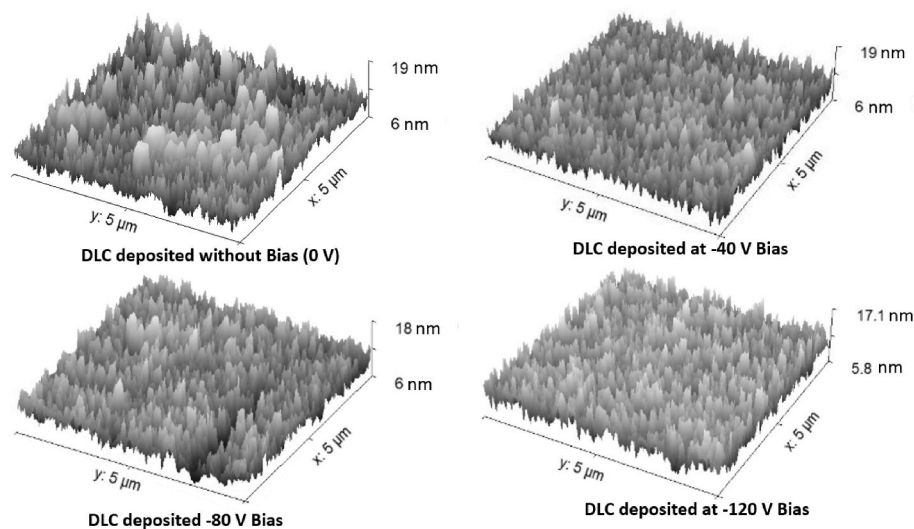**Fig. 2.** Surface roughness of DLC coatings deposited on glass substrates as a function of substrate bias voltage. All DLC coatings have a surface roughness (Ra) of less than 5 nm when measured across 25 μm^2. The surface roughness of DLC coatings reduces with increasing bias voltage.

contact angles when compared with the DLC coatings deposited with a substrate bias voltage of −40, −80, and −120 V. Surfaces with higher roughness have also demonstrated higher contact angles in literature reports [73]. The air molecules are trapped between the asperities and water drop which influences the surface contact angle [74]. The application of substrate bias relatively smoothens the surfaces, as reflected by their surface roughness, and corresponds to lower contact angles. A generic trend for a decrease in contact angle with an increase in bias voltage is also reported in the literature [71]. Similarly, the carbon phase compositions can also tune the water contact angle as a higher graphitic fraction by surface area or by carbon/carbon bonds have shown higher contact angles [75,76].

3.3. Mechanical properties of DLC coatings studied with nanoindentation

Fig. 4 presents the mechanical properties of DLC coatings measured with a nanoindenter against a bare glass substrate as a baseline reference. Contact depth, hardness and Young's modulus of the DLC coatings were measured as a function of their deposition bias voltage. Hardness is resistance to penetration [77]; hence contact depth is also an indirect measure of hardness. It can be seen that the DLC coating deposited without bias voltage (i.e., 0 V) has the least resistance to penetration and exhibits maximum contact depths of 35 nm when compared to other specimens. It can be observed that contact depth was gradually reduced

Fig. 4. Mechanical properties of DLC coatings deposited on glass substrates as a function of substrate bias voltage. DLC hardness increased by 12, 91, and 160% by applying a bias voltage of −40 V, −80 and −120 V while keeping all other deposition parameters the same.

with increasing bias voltage and measured as 31, 21 and 15 nm for −40 V, −80 V, and −120 V respectively. Similarly, the nano hardness of the DLC coatings was recorded as 7.8, 8.8, 14.9 and 20.3 GPa for 0, -40, −80, and −120 V, respectively. The DLC hardness increased with an increasing amount of carbon sp^3 bonds [51], hence, an increase of 12, 91, and 160% was observed at substrate bias of 40, -80, and −120 V. The increase in DLC coating hardness up to a threshold bias voltage is consistent with the literature [78,79]. Young's modulus of bias varied DLC coatings has a similar trend to hardness. The Young's modulus of the DLC coatings was 42, 52, 82 and 108 GPa at 0, -40, −80, and −120 V respectively. The stiffness probably increases due to the formation of a dense DLC structure with increasing bias voltage, as reported in the literature [80].

The application of bias voltage is well recognised to regulate DLC coating hardness. The increase in hardness of DLC coatings with bias voltage is well reported in previous literature studies [81,82] due to the increased electrostatic potential which in turn increases the plasma kinetics of carbon atoms and ions bombarding the substrate. These carbon atoms arriving with higher velocity produce a dense structure, and their disorder increases, promoting the formation of sp^3 bonds [83], which govern hardness, Young's modulus, and density of DLC coatings. The increase in disorder and carbon chain structure is also evident from the above-described Raman studies.

3.4. Biocompatibility measurements of hard and soft DLC coatings

Fig. 5A presents the absence of media measured at 570 and 600 nm wavelength, where L929 cells are exposed to 72 h and 168 h leached extracts for 72 h. Correspondingly, Fig. 5B shows the optical density of controls and DLC coatings measured after 72 h of exposure of L929 cells with 72 h and 168 h leached extracts. It can be seen that the optical density remained similar with a change in bias voltage for 72 h leaching extracts. However, a significant change in optical density could be observed when L929 cells were exposed to 168 h leached extracts of bias voltage and hardness varied DLC coatings after the same exposure time of 72 h. The soft DLC with the lowest hardness of 7.8 GPa deposited without any bias voltage retains an optical density the same as negative controls. However, the DLC coatings deposited with an increasing bias of −40, −80, and −120 V with hardness values of 8.8, 14.9, and 20.3 GPa respectively, lose their optical density compared to negative controls and the soft DLC coating deposited with zero bias. Optical density is an indirect indicator to estimate the biocompatibility on cell adhesion criteria [84] and higher optical densities refer to more adherent (living) cells as the dead cells are detached [85] from the surface and float in the media. The potential of single wavelength (570 nm) measurement as an indirect indicator of both cell morphology and adhesion, associated with MTT assay, is also reported in the literature [84].

Fig. 6 presents the L929 cell viability after 72 h treatment with 72 h and 168 h leached extracts of the DLC coatings and positive and negative controls. It can be observed that the Cu and DMSO positive controls have killed all L929 cells. And their cytotoxic response towards L929 cells is consistent with previous literature studies [86,87]. In comparison, the DMEM and medical-grade titanium negative controls and reference glass substrates retained their biocompatibility towards L929 cells irrespective of extract leaching times of 72 h and 168 h. All DLC coatings retained their biocompatibility for 72 h leached extracts. However, a variation in their biocompatibility appeared when the L929 cells were treated against 168 h extracts. The soft DLC coating retained its biocompatibility, whereas hard coatings came close to a cytotoxic regime, i.e. L929 cell viability of <70% of control [56].

The cell viability of the DLC coatings is attributed to carbon ion release rates, which mainly depend on carbon's amorphous or crystalline nature and their dimensional size. DLC wear debris have shown decreased cytotoxicity with increasing debris size in literature [88] as ion release rates are governed by the surface area [89,90]. Crystalline carbon nanomaterials [91] usually have higher carbon ion release rates,
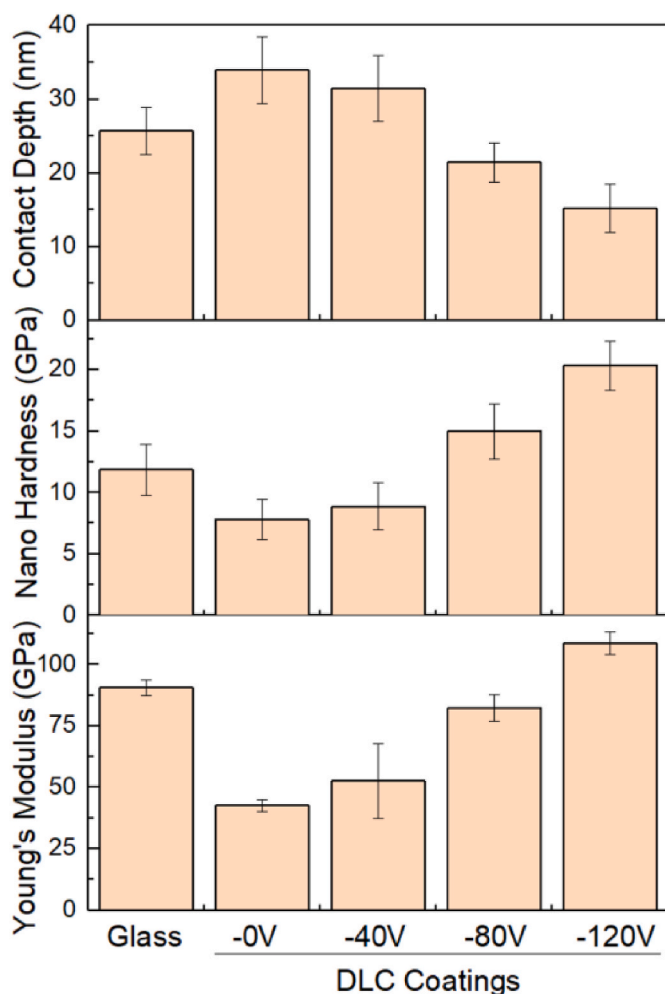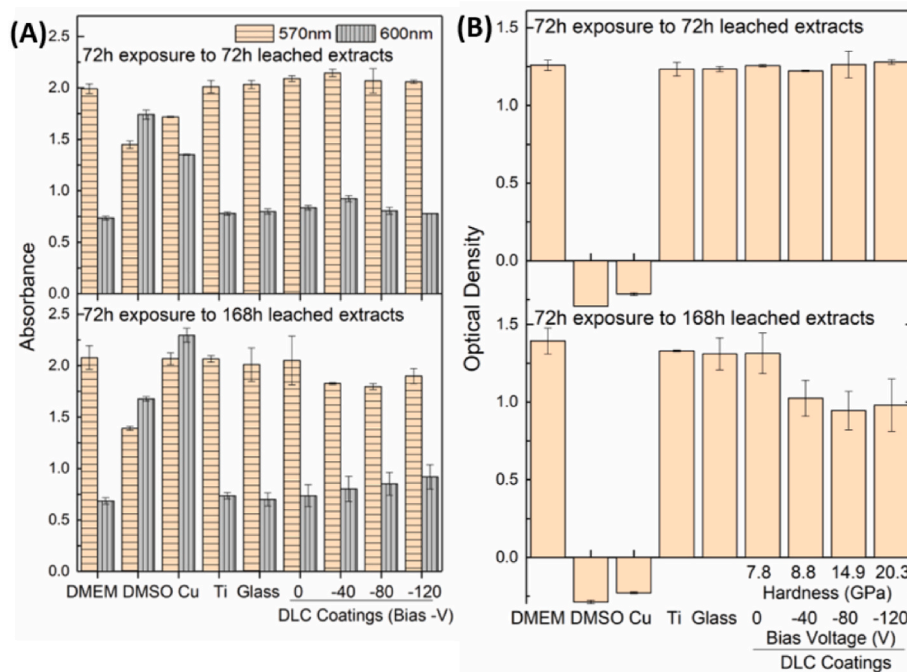
Fig. 5. (A) Absorbance and corresponding (B) Optical densities measured at 570 nm and 600 nm wavelengths after 72 h exposure of L929 cells against 72 h and 168 h leached extract of DLC coatings and control materials.
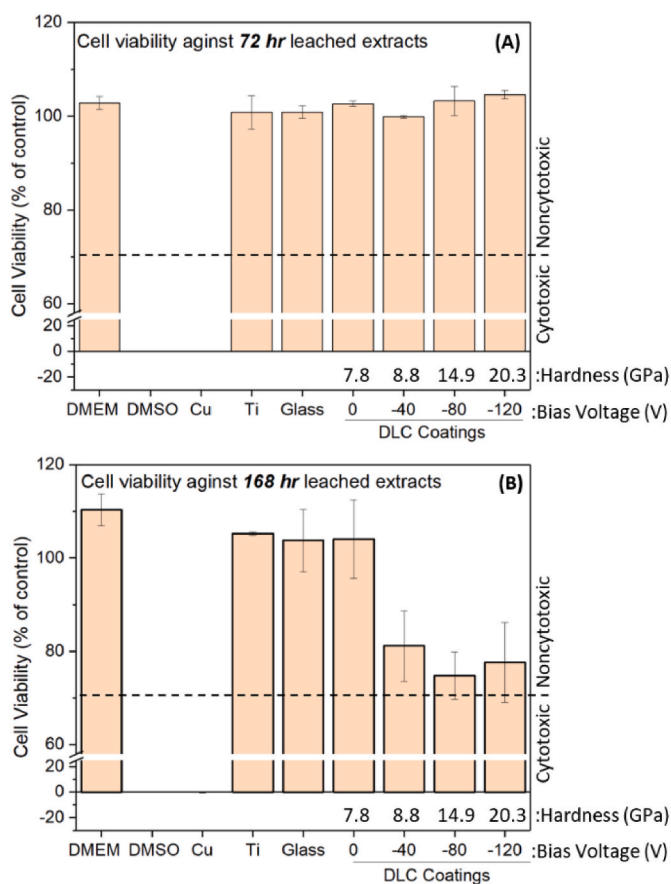

Fig. 6. L929 mouse fibroblast cells viability (% of control) against 72 h and 168 h leached extracts of hardness varied DLC coatings deposited as a function of bias voltage. Pure DMEM and medical-grade Ti were used as negative controls, DMSO and Cu were used as a positive control, and the laboratory-grade glass substrate was used as reference material.

increasing reactive oxygen species stimulating stresses, lipids peroxidation, and inflammation, leading to membrane damage of cells, proteins, and deoxyribonucleic acid. Therefore, most crystalline carbon nanomaterials are cytotoxic and used as germicide agents [92]. In contracts, pristine amorphous carbon coatings absorb fewer proteins and release less ions even when compared to doped DLC coatings [93], making them more suitable for biomedical applications. Amorphous DLC coatings have demonstrated a non-toxic response toward cells even with higher concentrations of 1.0 mg/mL [3,94]. The literature reflects that the graphitic structures have more cell viability than nanocrystalline structures such as carbon nanotubes [95]. Besides L929 cells, carbon materials with 70% sp^2 proportion have shown higher survival rates of Caco-2 cells when compared with carbon materials that have only 20% sp^2 characteristics [96]. These studies can correlate with our results, where soft DLC coatings with more sp^2 bonds have better cell viability than hard DLC coatings with relatively higher sp^3 bonds.

Fig. 7 presents the morphologies of L929 cells after 72 h interaction with 168 h leached extracts of DLC coatings and control materials. It is established that the living cells maintain a linear morphology while the dead cells become round [85]. The representative images, captured with a 10X lens microscope, show that the L929 cells have linear cellular morphologies and full cover the DLC coating surfaces in DMEM (Fig. 7A). In inset image presents the cell morphology at 400X optical zoom. Fig. 7B presents L929 cell interaction with Cu, a positive control. All cells have died with a change in their morphology from linear to round shape. Similarly, Fig. 7C and D presents the L929 cell interaction with soft DLC (0 V) and hard DLC (−120 V) coating surfaces and their leached extracts. The qualitative observation in the inset images presents that the living cell densities are relatively higher for the soft DLC than hard DLC coatings. Whereas the round–dead cells are relatively more observable in the hard DLC coating than soft DLC.

4. Summary

Table 1 summarises the outcomes of hardness varied DLC coatings prepared at bias voltages of 0, -40, −80, −120 V. Overall, the ID and IG peak position shifted upward, presenting an increase in disorder and
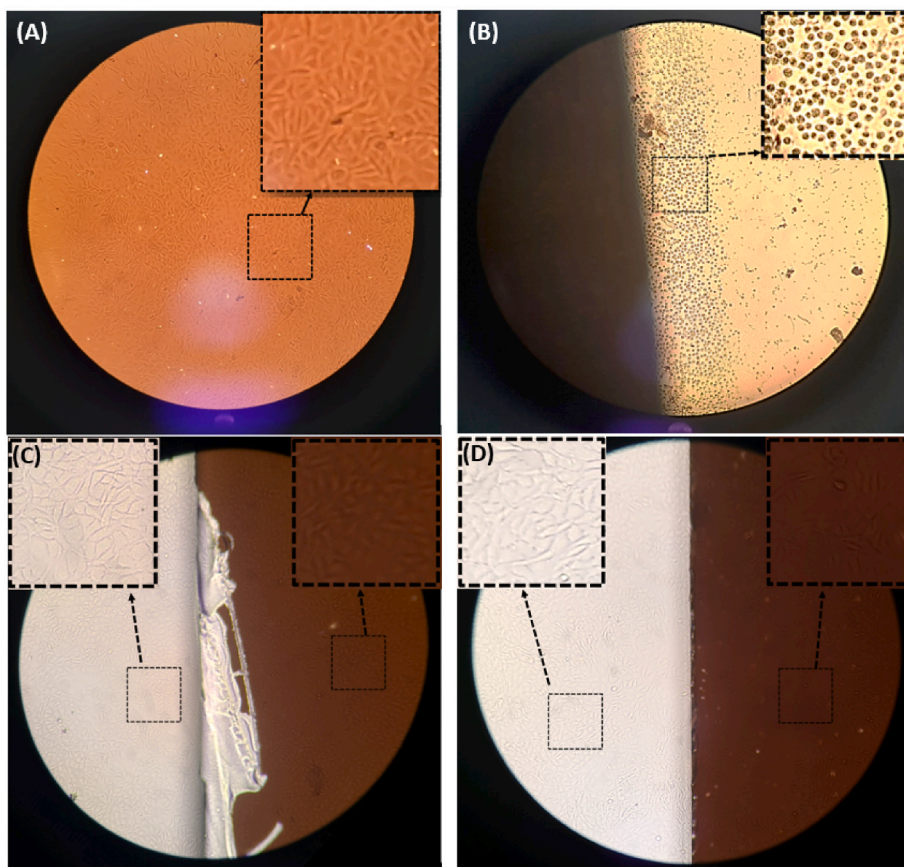
Fig. 7. Morphology of L929 mouse fibroblast observed with a microscope using 10X lens after 72 h exposure to 168 h leached extracts of control materials and DLC coatings. Representative images of L929 cells on (A) DLC coatings in DMEM – a negative control, (B) Copper – a positive control, (C) Soft DLC coating deposited without bias i.e., 0 V, and (D) Hard DLC coating deposited at −120 V. The inset images are optically zoomed at 400X. The left side inset (bright) images show L929 cells interaction with leached extracts and the right side inset (dark) images present L929 cells on the specimen surfaces.

Table 1
Correlation between mechanical properties and biocompatibility of DLC coatings.

Sr. No	Bias Voltage (V)	ID peak positions (cm^{-1})	IG peak positions (cm^{-1})	Contact Angle (θ)	Surface Roughness Ra (nm)	Hardness (GPa)	Young's Modulus (GPa)	Cell Viability % of control	
		SD 5% Maximum						72 h leached extracts	168 h leached extracts
1	0	1378.9	1525.3	76.1	2.33	7.8 ± 1.6	42.5 ± 2.5	102.6 ± 0.55	104.0 ± 8.39
2	−40	1394.5	1535.9	37.6	1.75	8.8 ± 1.9	52.5 ± 15.2	99.8 ± 0.25	81.1 ± 7.51
3	−80	1390.2	1531.9	64.9	1.76	14.9 ± 2.2	82.3 ± 5.3	103.2 ± 3.12	74.8 ± 5.06
4	−120	1388.3	1531.5	53.8	1.64	20.3 ± 1.9	108.5 ± 4.5	104.5 ± 0.86	77.5 ± 8.57

chain structure in the coatings with an increase in bias voltage. The contact angle and surface roughness overall reduce with an increase in bias voltage. The hardness and Young modulus increased with increasing bias voltage from 0 to −120 V. All DLC coatings remained biocompatible when 72 h leached extracts were treated against L929 cells. However, for 168 h leached extracts, the soft DLC coating having a hardness of 7.8 GPa, deposited at 0 V, retains excellent biocompatibility, similar to the negative titanium and glass controls. Whereas, the harder DLC coatings, i.e., 8.8–20.3 GPa deposited at −40 to −120 V, lose their biocompatibility and approach the cytotoxic regime of <70% cell viability.

5. Conclusions

Diamond-like carbon (DLC) coatings were sputter deposited as a function of bias voltage at 0, -40, −80, and −140 V. The disorder in atomic structure and carbon chain structure in the coating increases with increasing bias voltage. The DLC coatings have hardness values of 7.8, 8.8, 14.9, and 20.3 GPa when deposited at bias voltages of 0, -40,

−80, and −140 V respectively. The biocompatibility of DLC coatings was assessed against L929 mouse fibroblast cells and it was observed that the soft DLC coatings deposited without bias and having a hardness of 7.8 GPa remained biocompatible irrespective of extract leaching time of 72 h or 168 h. Whereas DLC coatings deposited between −40 and −120 V, having a hardness values between 8.8 and 20.3 GPa, remained biocompatible for 72 h leached extracts only and approached a cytotoxic regime when L929 cells were treated against their 168 h leached extracts. The work concludes with the following remarks.

- All DLC coatings are biocompatible, but hard DLC coatings may lose biocompatibility earlier than soft DLC coatings and may become toxic to the implant host, correspondingly reducing product life, posing revision surgery, and economical and sustainability challenges.
- Not all invasive implants need hard DLC coatings. Non-load carrying invasive implants may be coated with softer DLC as long as it fulfils all other specific requirements. Hard DLC coatings are desirous for

bio-mechanical actions such as bearing surfaces of invasive implants to improve tribological performance.

- The effect of surface area, density, dimensional features, and porosity of pure DLC coatings is not yet systemically investigated against cell viability response of amorphous DLC coatings. Such investigations are likely to support appropriate selection of DLC coatings for specific biomedical applications.

Funding

Note

The referred intellectual property rights and commercial tradenames and products in this work are up to the best of author's knowledge and search.

Data availability statements

The datasets generated during and/or analysed during the current study are available in the [Figshare] repository, [DOI: 10.25398/rd. northumbria.21393960].

Declaration of competing interest

The authors declare that they have no known competing financial interests or personal relationships that could have appeared to influence the work reported in this paper.

References

[1] J. Czarnecka, M. Wiśniewski, N. Forbot, P. Bolibok, A.P. Terzyk, K. Roszek, Cytotoxic or not? Disclosing the toxic nature of carbonaceous nanomaterials through, Nano–Bio Interactions, Materials 13 (9) (2020).

[2] C. Popov, W. Kulisch, J.P. Reithmaier, T. Dostalova, M. Jelinek, N. Anspach, C. Hammann, Bioproperties of nanocrystalline diamond/amorphous carbon composite films, Diam. Relat. Mater. 16 (4) (2007) 735–739.

[3] R. Olivares, S.E. Rodil, H. Arzate, Osteoinduction properties of graphite-like amorphous carbon films evaluated in-vitro, Diam. Relat. Mater. 16 (10) (2007) 1858–1867.

[4] K.-L. Ou, C.-C. Weng, E. Sugiatno, M. Ruslin, Y.-H. Lin, H.-Y. Cheng, Effect of nanostructured thin film on minimally invasive surgery devices applications: characterization, cell cytotoxicity evaluation and an animal study in rat, Surg. Endosc. 30 (7) (2016) 3035–3049.

[5] H.S. Tran, M.M. Puc, C.W. Hewitt, D.B. Soll, S.W. Marra, V.A. Simonetti, J. H. Cilley, A.J. DelRossi, Diamond-like carbon coating and plasma or glow discharge treatment of mechanical heart valves, J. Invest. Surg. 12 (3) (1999) 133–140.

[6] Y. Ohgoe, S. Takada, K.K. Hirakuri, K. Tsuchimoto, A. Homma, T. Miyamatsu, T. Saitou, G. Friedbacher, E. Tatsumi, Y. Taenaka, Y. Fukui, Investigating the functionality of diamond-like carbon films on an artificial heart diaphragm, Am. Soc. Artif. Intern. Organs J. 49 (6) (2003).

[7] K. Gutensohn, C. Beythien, J. Bau, T. Fenner, P. Grewe, R. Koester, K. Padmanaban, P. Kuehnl, In vitro analyses of diamond-like carbon coated stents: reduction of metal ion release, platelet activation, and thrombogenicity, Thromb. Res. 99 (6) (2000) 577–585.

[8] S. Watari, K. Wada, M. Araki, T. Sadahira, D. Ousaka, S. Oozawa, T. Nakatani, Y. Imai, J. Kato, R. Kariyama, Intraluminal diamond-like carbon coating with anti-adhesion and anti-biofilm effects for uropathogens: a novel technology applicable to urinary catheters, Int. J. Urol. 28 (12) (2021) 1282–1289.

[9] S. Kobayashi, Y. Ohgoe, K. Ozeki, K. Sato, T. Sumiya, K.K. Hirakuri, H. Aoki, Diamond-like carbon coatings on orthodontic archwires, Diam. Relat. Mater. 14 (3) (2005) 1094–1097.

[10] S. Kobayashi, Y. Ohgoe, K. Ozeki, K. Hirakuri, H. Aoki, Dissolution effect and cytotoxicity of diamond-like carbon coatings on orthodontic archwires, J. Mater. Sci. Mater. Med. 18 (12) (2007) 2263–2268.

[11] H. Hosotani, Physical properties of an intraocular lens coated with diamond-like carbon film, Nippon. Ganka Gakkai Zasshi 101 (11) (1997) 841–846.

[12] B. Rothammer, K. Neusser, M. Marian, M. Bartz, S. Krauß, T. Böhm, S. Thiele, B. Merle, R. Detsch, S. Wartzack, Amorphous carbon coatings for total knee replacements—Part I: deposition, cytocompatibility, chemical and mechanical properties, Polymers 13 (12) (2021).

[13] C. Skjöldebrand, J.L. Tipper, P. Hatto, M. Bryant, R.M. Hall, C. Persson, Current status and future potential of wear-resistant coatings and articulating surfaces for hip and knee implants, Materials Today Bio 15 (2022), 100270.

[14] V.-M. Tiainen, Amorphous carbon as a bio-mechanical coating — mechanical properties and biological applications, Diam. Relat. Mater. 10 (2) (2001) 153–160.

[15] A.W. Zia, M. Birkett, Deposition of diamond-like carbon coatings: conventional to non-conventional approaches for emerging markets, Ceram. Int. 47 (20) (2021) 28075–28085.

[16] H. Schmellenmeier, Die Beeinflussung von festen Oberflachen durch eine ionisierte, Exp. Tech. Phys. 1 (1953) 49–68.

[17] S. Aisenberg, R. Chabot, Ion-beam deposition of thin films of diamondlike carbon, J. Appl. Phys. 42 (7) (1971) 2953–2958.

[18] M. Kano, Diamond-like carbon coating applied to automotive engine components, Tribol. Online 9 (3) (2014) 135–142.

[19] P.S. Martins, P.A.A.M. Júnior, J.R.G. Carneiro, E.C.T. Ba, V.F. Vieira, Study of Diamond-Like Carbon coating application on carbide substrate for cutting tools used in the drilling process of an Al–Si alloy at high cutting speeds, Wear 498 (2022), 204326.

[20] W. Milne, Electronic devices from diamond-like carbon, Semicond. Sci. Technol. 18 (3) (2003) S81.

[21] B. Cortese, D. Caschera, F. Federici, G.M. Ingo, G. Gigli, Superhydrophobic fabrics for oil–water separation through a diamond like carbon (DLC) coating, J. Mater. Chem. 2 (19) (2014) 6781–6789.

[22] W.S. Choi, K. Kim, J. Yi, B. Hong, Diamond-like carbon protective anti-reflection coating for Si solar cell, Mater. Lett. 62 (4–5) (2008) 577–580.

[23] L.A. Thomson, F.C. Law, N. Rushton, J. Franks, Biocompatibility of diamond-like carbon coating, Biomaterials 12 (1) (1991) 37–40.

[24] R. Hauert, A review of modified DLC coatings for biological applications, Diam. Relat. Mater. 12 (3) (2003) 583–589.

[25] R.K. Roy, K.-R. Lee, Biomedical applications of diamond-like carbon coatings: a review, J. Biomed. Mater. Res. B Appl. Biomater. 83B (1) (2007) 72–84.

[26] A. Grill, Diamond-like carbon coatings as biocompatible materials—an overview, Diam. Relat. Mater. 12 (2) (2003) 166–170.

[27] A. Almaguer-Flores, R. Olivares-Navarrete, A. Lechuga-Bernal, L.A. Ximénez-Fyvie, S.E. Rodil, Oral bacterial adhesion on amorphous carbon films, Diam. Relat. Mater. 18 (9) (2009) 1179–1185.

[28] I. Dion, X. Roques, C. Baquey, E. Baudet, B. Basse Cathalinat, N. More, Hemocompatibility of diamond-like carbon coating, Bio Med. Mater. Eng. 3 (1) (1993) 51–55.

[29] C.C. Wachesk, S.H. Seabra, T.A.T. Dos Santos, V.J. Trava-Airoldi, A.O. Lobo, F. R. Marciano, In vivo biocompatibility of diamond-like carbon films containing TiO2 nanoparticles for biomedical applications, J. Mater. Sci. Mater. Med. 32 (9) (2021) 117.

[30] M.I. Jones, I.R. McColl, D.M. Grant, K.G. Parker, T.L. Parker, Protein adsorption and platelet attachment and activation, on TiN, TiC, and DLC coatings on titanium for cardiovascular applications, J. Biomed. Mater. Res. 52 (2) (2000) 413–421.

[31] G. Taeger, L.E. Podleska, B. Schmidt, M. Ziegler, D. Nast-Kolb, Comparison of diamond-like-carbon and alumina-oxide articulating with polyethylene in total hip arthroplasty, Mater. Werkst. 34 (12) (2003) 1094–1100.

[32] D.P. Dowling, P.V. Kola, K. Donnelly, T.C. Kelly, K. Brumitt, L. Lloyd, R. Eloy, M. Therin, N. Weill, Evaluation of diamond-like carbon-coated orthopaedic implants, Diam. Relat. Mater. 6 (2) (1997) 390–393.

[33] F.Z. Cui, D.J. Li, A review of investigations on biocompatibility of diamond-like carbon and carbon nitride films, Surf. Coating. Technol. 131 (1) (2000) 481–487.

[34] R. Matsumoto, K. Sato, K. Ozeki, K. Hirakuri, Y. Fukui, Cytotoxicity and tribological property of DLC films deposited on polymeric materials, Diam. Relat. Mater. 17 (7) (2008) 1680–1684.

[35] C. Hinüber, C. Kleemann, R.J. Friederichs, L. Haubold, H.J. Scheibe, T. Schuelke, C. Boehlert, M.J. Baumann, Biocompatibility and mechanical properties of diamond-like coatings on cobalt-chromium-molybdenum steel and titanium-aluminum-vanadium biomedical alloys, J. Biomed. Mater. Res. 95A (2) (2010) 388–400.

[36] D. Sheeja, B.K. Tay, L.N. Nung, Feasibility of diamond-like carbon coatings for orthopaedic applications, Diam. Relat. Mater. 13 (1) (2004) 184–190.

[37] C. Hinüber, C. Kleemann, R.J. Friederichs, L. Haubold, H.J. Scheibe, T. Schuelke, C. Boehlert, M.J. Baumann, Biocompatibility and mechanical properties of diamond-like coatings on cobalt-chromium-molybdenum steel and titanium-aluminum-vanadium biomedical alloys, J. Biomed. Mater. Res. 95 (2) (2010) 388–400.

[38] D. Bociaga, M. Kaminska, A. Sobczyk-Guzenda, K. Jastrzebski, L. Swiatek, A. Olejnik, Surface properties and biological behaviour of Si-DLC coatings fabricated by a multi-target DC–RF magnetron sputtering method for medical applications, Diam. Relat. Mater. 67 (2016) 41–50.

[39] S.E. Rodil, R. Olivares, H. Arzate, In vitro cytotoxicity of amorphous carbon films, Bio Med. Mater. Eng. 15 (1–2) (2005) 101–112.

[40] J. Li, Z. Li, J. Tu, G. Jin, L. Li, K. Wang, H. Wang, In vitro and in vivo investigations of a-C/a-C:Ti nanomultilayer coated Ti6Al4V alloy as artificial femoral head, Mater. Sci. Eng. C 99 (2019) 816–826.

[41] L. Li, W. Bai, X. Wang, C. Gu, G. Jin, J. Tu, Mechanical properties and in vitro and in vivo biocompatibility of a-C/a-C:Ti nanomultilayer films on Ti6Al4V alloy as medical implants, ACS Appl. Mater. Interfaces 9 (19) (2017) 15933–15942.

[42] M. Fedel, A. Motta, D. Maniglio, C. Migliaresi, Surface properties and blood compatibility of commercially available diamond-like carbon coatings for cardiovascular devices, J. Biomed. Mater. Res. B Appl. Biomater. 90B (1) (2009) 338–349.

[43] R. Olivares, S.E. Rodil, H. Arzate, In vitro studies of the biomineralization in amorphous carbon films, Surf. Coating. Technol. 177–178 (2004) 758–764.

[44] E.T. Uzumaki, C.S. Lambert, A.R. Santos, C.A.C. Zavaglia, Surface properties and cell behaviour of diamond-like carbon coatings produced by plasma immersion, Thin Solid Films 515 (1) (2006) 293–300.

[45] A. Singh, G. Ehteshami, S. Massia, J. He, R.G. Storer, G. Raupp, Glial cell and fibroblast cytotoxicity study on plasma-deposited diamond-like carbon coatings, Biomaterials 24 (28) (2003) 5083–5089.

[46] J.Y. Chen, L.P. Wang, K.Y. Fu, N. Huang, Y. Leng, Y.X. Leng, P. Yang, J. Wang, G. J. Wan, H. Sun, X.B. Tian, P.K. Chu, Blood compatibility and sp3/sp2 contents of diamond-like carbon (DLC) synthesized by plasma immersion ion implantation-deposition, Surf. Coating. Technol. 156 (1) (2002) 289–294.

[47] J.L. Endrino, R. Escobar Galindo, H.S. Zhang, M. Allen, R. Gago, A. Espinosa, A. Anders, Structure and properties of silver-containing a-C(H) films deposited by plasma immersion ion implantation, Surf. Coating. Technol. 202 (15) (2008) 3675–3682.

[48] H. Zhou, L. Xu, A. Ogino, M. Nagatsu, Investigation into the antibacterial property of carbon films, Diam. Relat. Mater. 17 (7) (2008) 1416–1419.

[49] K.H. Lee, S.H. Lee, R.S. Ruoff, Synthesis of diamond-like carbon nanofiber films, ACS Nano 14 (10) (2020) 13663–13672.

[50] I. Hutchings, P. Shipway, 7 - surface engineering, in: I. Hutchings, P. Shipway (Eds.), Tribology, second ed., Butterworth-Heinemann, 2017, pp. 237–281.

[51] N. Ohtake, M. Hiratsuka, K. Kanda, H. Akasaka, M. Tsujioka, K. Hirakuri, A. Hirata, T. Ohana, H. Inaba, M. Kano, H. Saitoh, Properties and classification of diamond-like carbon films, Materials 14 (2) (2021) 315.

[52] K.N. Pandiyaraj, V. Selvarajan, J. Heeg, F. Junge, A. Lampka, T. Barfels, M. Wienecke, Y.H. Rhee, H.W. Kim, Influence of bias voltage on diamond like carbon (DLC) film deposited on polyethylene terephthalate (PET) film surfaces using PECVD and its blood compatibility, Diam. Relat. Mater. 19 (7) (2010) 1085–1092.

[53] V. Zavaleyev, J. Walkowicz, M. Sawczak, D. Moszyński, J. Ryl, Effect of substrate bias on the properties of DLC films created using a combined vacuum arc, Bull. Mater. Sci. 44 (3) (2021) 170.

[54] W. Jing, L. Gui-Chang, W. Li-Da, D. Xin-Lü, X. Jun, Studies of diamond-like carbon (DLC) films deposited on stainless steel substrate with Si/SiC intermediate layers, Chin. Phys. B 17 (8) (2008) 3108–3114.

[55] C.C. Lukose, I. Anestopoulos, T. Mantso, L. Bowen, M.I. Panayiotidis, M. Birkett, Thermal activation of Ti(1-x)Au(x) thin films with enhanced hardness and biocompatibility, Bioact. Mater. 15 (2022) 426–445.

[56] V. Cannella, R. Altomare, G. Chiaramonte, S. Di Bella, F. Mira, L. Russotto, P. Pisano, A. Guercio, Cytotoxicity evaluation of endodontic pins on L929 cell line, BioMed Res. Int. (2019), 3469525, 2019.

[57] S. Movahed, A.K. Nguyen, P.L. Goering, S.A. Skoog, R.J. Narayan, Argon and oxygen plasma treatment increases hydrophilicity and reduces adhesion of silicon-incorporated diamond-like coatings, Biointerphases 15 (4) (2020), 041007.

[58] M. Singh, R.K. Singh, S.K. Singh, S.K. Mahto, N. Misra, In vitro biocompatibility analysis of functionalized poly(vinyl chloride)/layered double hydroxide nanocomposites, RSC Adv. 8 (71) (2018) 40611–40620.

[59] A.C. Ferrari, J. Robertson, Interpretation of Raman spectra of disordered and amorphous carbon, Phys. Rev. B 61 (20) (2000) 14095–14107.

[60] S.M. Fayed, H. Wu, D. Chen, S. Li, Y. Zhou, H. Wang, M.M. Sadawy, Influence of positive pulse voltages on structure, mechanical, and corrosion inhibition characteristics of Si/DLC coatings, Surf. Coating. Technol. 445 (2022), 128749.

[61] A.C. Ferrari, J. Robertson, A.C. Ferrari, J. Robertson, Raman spectroscopy of amorphous, nanostructured, diamond–like carbon, and nanodiamond, Philos. Trans. R. Soc. London, Ser. A: Math. Phys. Eng. Sci. 362 (1824) (2004) 2477–2512.

[62] A.W. Zia, Z. Zhou, L.K.-Y. Li, Chapter 7 - structural, mechanical, and tribological characteristics of diamond-like carbon coatings, in: P. Nguyen Tri, S. Rtimi, C. M. Ouellet Plamondon (Eds.), Nanomaterials-Based Coatings, Elsevier, 2019, pp. 171–194.

[63] J.C. Ding, M. Chen, H. Mei, S. Jeong, J. Zheng, Y. Yang, Q. Wang, K.H. Kim, Microstructure, mechanical, and wettability properties of Al-doped diamond-like films deposited using a hybrid deposition technique: bias voltage effects, Diam. Relat. Mater. 123 (2022), 108861.

[64] P.W. May, J.A. Smith, K.N. Rosser, 785 nm Raman spectroscopy of CVD diamond films, Diam. Relat. Mater. 17 (2) (2008) 199–203.

[65] A.C. Ferrari, Raman spectroscopy of graphene and graphite: disorder, electron–phonon coupling, doping and nonadiabatic effects, Solid State Commun. 143 (1) (2007) 47–57.

[66] J. Peng, Y. Peng, Y. Xiao, J. Liao, J. Huang, X. Qiu, L. Li, Effect of cryogenic pretreatments on the microstructure and mechanical performance of diamond-like carbon coatings for high-speed alloys, Diam. Relat. Mater. 127 (2022), 109189.

[67] H. Cao, X. Ye, H. Li, F. Qi, Q. Wang, X. Ouyang, N. Zhao, B. Liao, Microstructure, mechanical and tribological properties of multilayer Ti-DLC thick films on Al alloys by filtered cathodic vacuum arc technology, Mater. Des. 198 (2021), 109320.

[68] G. Liu, Z. Wen, K. Chen, L. Dong, Z. Wang, B. Zhang, L. Qiang, Optimizing the microstructure, mechanical, and tribological properties of Si-DLC coatings on NBR rubber for its potential applications, Coatings 10 (7) (2020) 671.

[69] L. Wang, L. Li, X. Kuang, Effect of substrate bias on microstructure and mechanical properties of WC-DLC coatings deposited by HiPIMS, Surf. Coating. Technol. 352 (2018) 33–41.

[70] R. Hu, J. Tang, G. Zhu, Q. Deng, J. Lu, The effect of duty cycle and bias voltage for graphite-like carbon film coated 304 stainless steel as metallic bipolar plate, J. Alloys Compd. 772 (2019) 1067–1078.

[71] W. Dai, H. Zheng, G. Wu, A. Wang, Effect of bias voltage on growth property of Cr-DLC film prepared by linear ion beam deposition technique, Vacuum 85 (2) (2010) 231–235.

[72] P. Yang, N. Huang, Y.X. Leng, Z.Q. Yao, H.F. Zhou, M. Maitz, Y. Leng, P.K. Chu, Wettability and biocompatibility of nitrogen-doped hydrogenated amorphous carbon films: effect of nitrogen, Nucl. Instrum. Methods Phys. Res. Sect. B Beam Interact. Mater. Atoms 242 (1) (2006) 22–25.

[73] S.A. Mahadik, F. Pedraza, S.S. Mahadik, B.P. Relekar, S.S. Thorat, Biocompatible superhydrophobic coating material for biomedical applications, J. Sol. Gel Sci. Technol. 81 (3) (2017) 791–796.

[74] A.W. Zia, Y.-Q. Wang, S. Lee, Effect of physical and chemical plasma etching on surface wettability of carbon fiber–reinforced polymer composites for bone plate applications, Adv. Polym. Technol. 34 (1) (2015).

[75] S.K. Behera, A. Kumar P, N. Dogra, M. Nosonovsky, P. Rohatgi, Effect of microstructure on contact angle and corrosion of ductile iron: iron–graphite composite, Langmuir 35 (49) (2019) 16120–16129.

[76] X. Rao, J. Yang, Z. Chen, Y. Yuan, Q. Chen, X. Feng, L. Qin, Y. Zhang, Tuning C–C sp2/sp3 ratio of DLC films in FCVA system for biomedical application, Bioact. Mater. 5 (2) (2020) 192–200.

[77] N. Efron, 11 - rigid lens materials, in: N. Efron (Ed.), Contact Lens Practice, third ed., Elsevier, 2018, pp. 115–122.e1.

[78] M.S. Kabir, Z. Zhou, Z. Xie, P. Munroe, Designing multilayer diamond like carbon coatings for improved mechanical properties, J. Mater. Sci. Technol. 65 (2021) 108–117.

[79] L. Wang, Y. Liu, H. Chen, M. Wang, Nanoindentation-induced deformation behaviors of tetrahedral amorphous carbon film deposited by cathodic vacuum arc with different substrate bias voltages, Appl. Surf. Sci. 576 (2022), 151741.

[80] S. Ponce, N.Z. Calderon, J.L. Ampuero, A. La Rosa-Toro, A. Talledo, W. Gacitúa, B. R. Pujada, Influence of the substrate bias on the stress in Ti-DLC films deposited by dc magnetron sputtering, J. Phys. Conf. 1558 (1) (2020), 012009.

[81] K. Yamamoto, K. Matsukado, Effect of hydrogenated DLC coating hardness on the tribological properties under water lubrication, Tribol. Int. 39 (12) (2006) 1609–1614.

[82] J.C. Ding, H. Mei, S. Jeong, J. Zheng, Q.M. Wang, K.H. Kim, Effect of bias voltage on the microstructure and properties of Nb-DLC films prepared by a hybrid sputtering system, J. Alloys Compd. 861 (2021), 158505.

[83] N.-T. Do, V.-H. Dinh, L.V. Lich, H.-H. Dang-Thi, T.-G. Nguyen, Effects of substrate bias voltage on structure of diamond-like carbon films on aisi 316L stainless steel: a molecular dynamics simulation study, Materials 14 (17) (2021).

[84] F.P. Lee, D.Y. Wang, L.K. Chen, C.M. Kung, Y.C. Wu, K.L. Ou, C.H. Yu, Antibacterial nanostructured composite films for biomedical applications: microstructural characteristics, biocompatibility, and antibacterial mechanisms, Biofouling 29 (3) (2013) 295–305.

[85] A. Isakovic, Z. Markovic, B. Todorovic-Markovic, N. Nikolic, S. Vranjes-Djuric, M. Mirkovic, M. Dramicanin, L. Harhaji, N. Raicevic, Z. Nikolic, V. Trajkovic, Distinct cytotoxic mechanisms of pristine versus hydroxylated fullerene, Toxicol. Sci. 91 (1) (2006) 173–183.

[86] G. Arena, G. Maccarrone, E. Rizzarelli, S. Sciuto, M. Bindoni, V. Cardile, M. C. Riello, E. Rizzarelli, Cytotoxic and cytostatic activity of copper(II) complexes. Importance of the speciation for the correct interpretation of the in vitro biological results, J. Inorg. Biochem. 50 (1) (1993) 31–45.

[87] Y.J. Wu, Y.C. Wu, I.F. Chen, Y.-L. Wu, C.W. Chuang, H.H. Huang, S.M. Kuo, Reparative effects of astaxanthin-hyaluronan nanoaggregates against retrorsine-CCl4-induced liver fibrosis and necrosis, Molecules 23 (4) (2018).

[88] T.T. Liao, Q.Y. Deng, S.S. Li, X. Li, L. Ji, Q. Wang, Y.X. Leng, N. Huang, Evaluation of the size-dependent cytotoxicity of DLC (diamondlike carbon) wear debris in arthroplasty applications, ACS Biomater. Sci. Eng. 3 (4) (2017) 530–539.

[89] W. Zhang, Y. Yao, N. Sullivan, Y. Chen, Modeling the primary size effects of citrate-coated silver nanoparticles on their ion release kinetics, Environ. Sci. Technol. 45 (10) (2011) 4422–4428.

[90] M.F. Gencoglu, A. Spurri, M. Franko, J. Chen, D.K. Hensley, C.L. Heldt, D. Saha, Biocompatibility of soft-templated mesoporous carbons, ACS Appl. Mater. Interfaces 6 (17) (2014) 15068–15077.

[91] X. Yuan, X. Zhang, L. Sun, Y. Wei, X. Wei, Cellular toxicity and immunological effects of carbon-based nanomaterials, Part. Fibre Toxicol. 16 (1) (2019) 18.

[92] Á. Serrano-Aroca, K. Takayama, A. Tuñón-Molina, M. Seyran, S.S. Hassan, P. Pal Choudhury, V.N. Uversky, K. Lundstrom, P. Adadi, G. Palù, A.A.A. Aljabali, G. Chauhan, R. Kandimalla, M.M. Tambuwala, A. Lal, T.M. Abd El-Aziz, S. Sherchan, D. Barh, E.M. Redwan, N.G. Bazan, Y.K. Mishra, B.D. Uhal, A. Brufsky, Carbon-based nanomaterials: promising antiviral agents to combat COVID-19 in the microbial-resistant era, ACS Nano 15 (5) (2021) 8069–8086.

[93] N.K. Manninen, S. Calderon, I. Carvalho, M. Henriques, A. Cavaleiro, S. Carvalho, Antibacterial Ag/a-C nanocomposite coatings: the influence of nano-galvanic a-C and Ag couples on Ag ionization rates, Appl. Surf. Sci. 377 (2016) 283–291.

[94] S. Jain, A. Sharma, B. Basu, In vitro cytocompatibility assessment of amorphous carbon structures using neuroblastoma and Schwann cells, J. Biomed. Mater. Res. B Appl. Biomater. 101 (4) (2013) 520–531.

[95] M. Rezazadeh Azari, Y. Mohammadian, Comparing in vitro cytotoxicity of graphite, short multi-walled carbon nanotubes, and long multi-walled carbon nanotubes, Environ. Sci. Pollut. Control Ser. 27 (13) (2020) 15401–15406.

[96] D. Saha, C.L. Heldt, M.F. Gencoglu, K.S. Vijayaragavan, J. Chen, A. Saksule, A study on the cytotoxicity of carbon-based materials, Mater. Sci. Eng. C 68 (2016) 101–108.